Biometals (2010) 23:1139–1147
DOI 10.1007/s10534-010-9363-8

Inhibition protein tyrosine phosphatases by an oxovanadium glutamate complex, $Na_2[VO(Glu)_2(CH_3OH)]$(Glu = glutamate)

Liping Lu · Sulian Wang · Miaoli Zhu · Zhiwei Liu · Maolin Guo · Shu Xing · Xueqi Fu

Received: 18 January 2010 / Accepted: 23 June 2010 / Published online: 9 July 2010

Abstract The insulin-sensitizing effect of vanadium complexes has been linked to their ability to inhibit protein tyrosine phosphatases (PTPs). Considering that vanadium complexes may exchange in vivo with amino acids, forming in situ vanadium–amino acid complexes, we have synthesized and characterized an oxovanadium glutamate complex, $Na_2[V(IV)O(Glu)_2(CH_3OH)]H_2O$ (**1**·H_2O). The complex showed potent inhibition against four human PTPs (PTP1B, TCPTP, HePTP, and SHP-1) with IC_{50} in the 0.21–0.37 μM ranges. Fluorescence titration studies suggest that the complex binds to PTP1B with the formation of a 2:1 complex. Enzyme kinetics analysis using Lineweaver–Burk plots indicates a typical competitive inhibition mode.

Keywords Protein tyrosine phosphatases · Inhibition · Oxovanadium–glutamate complex · Fluorescence

L. Lu · S. Wang · M. Zhu (✉)
Institute of Molecular Science, Key Laboratory of Chemical Biology and Molecular Engineering of the Education Ministry, Shanxi University, Taiyuan 030006, Shanxi, People's Republic of China
e-mail: miaoli@sxu.edu.cn

Z. Liu · M. Guo (✉)
Department of Chemistry and Biochemistry, University of Massachusetts, Dartmouth 02747, MA, USA
e-mail: mguo@umassd.edu

S. Xing · X. Fu (✉)
Edmond H. Fischer Signal Transduction Laboratory, College of Life Sciences, Jilin University, Changchun 130023, People's Republic of China
e-mail: fxq@jlu.edu.cn

M. Zhu
State Key Laboratory of Coordination Chemistry, Nanjing University, Nanjing 210093, People's Republic of China

Introduction

Protein tyrosine phosphatases (PTPs) are a family of diverse enzymes that regulate various cellular processes by a common dephosphorylation catalytic mechanism (Andersen et al. 2004). Dysregulation of PTP activities contributes to the pathogenesis of several human diseases, including diabetes, obesity, cancer, and immune disorders (Andersen et al. 2004; Arena et al. 2005; Zhang 2001). Among various members in the PTP superfamily, protein tyrosine phosphatase 1B(PTP1B) has been demonstrated as a key negative regulator of insulin signaling and emerged as an attractive target for the treatment of type II diabetes. PTP1B directly inactivates the insulin receptor (IR) by dephosphorylating tyrosine residues in the regulatory domain (Kenner et al. 1996; Saltiel and Kahn 2001). Overexpression of PTP1B inhibits insulin signaling (Byon et al. 1998). PTP1B gene knockout or antisense studies in normal and diabetic mice have shown lowered blood glucose levels and improved insulin responsiveness through

enhanced IR signaling in peripheral tissues (Elchebly et al. 1999; Klaman et al. 2000; Zinker et al. 2002). Therefore, PTP1B inhibitors have been pursued to develop novel anti-diabetic drugs (Xie and Seto 2007; Na et al. 2006; Alal et al. 2006; Shrestha et al. 2007; Sparks et al. 2007; Maccari et al. 2007; Winter et al. 2005).

Inorganic salts of the trace element vanadium have been demonstrated to imitate actions of insulin (Heyliger et al. 1985). Comparing to inorganic vanadium salts, complexes of vanadium with appropriate organic ligands can improve absorption, tissue uptake, potency, and decrease toxicity of the metal (McNeill et al. 1995). An organic vanadyl derivative [bis(maltolato)oxovanadium(IV)] (BMOV) is currently on phase II clinical trials as an anti-diabetic drug (Mukherjee et al. 2008). The mechanism of action for vanadium's insulin-sensitizing effects has not been well understood but association with inhibition of protein tyrosine phosphatases has been implicated (Peters et al. 2003; Crans et al. 2004). Vanadium compounds have been shown to directly inhibit some PTPs including PTP1B (Posner et al. 1994; Huyer et al. 1997; Nxumalo et al. 1998; Peters et al. 2003; Yuan. et al. 2009, 2010; Gao et al. 2009; Lu et al. submitted). When vanadium salts or vanadium complexes enter the body, they may undergo ligand exchange with other biologically available small ligands such as amino acids, forming in situ vanadium complexes with these bioligands. The inhibitory effects of vanadium complexes with small bioligands on PTPs thus attracted our interest. In this paper, we investigated the inhibitory effects of $Na_2[VO(Glu)_2(CH_3OH)]\cdot H_2O$ (**1**·H_2O) on four human PTPs and the more detailed interactions between the vanadium complex and PTP1B.

Materials and methods

Materials

L-Glutamic acid (H_2Glu) was purchased commercially without further purification. Other chemicals and solvents are AR grade and were purchased commercially and used without further purification. PTP1B, T-cell protein tyrosine phosphatase (TCPTP), Src homology phosphatase 1 (SHP-1), and hematopoietic tyrosine phosphatase (HePTP) were expressed and purified as described previously (Yuan et al. 2009; Lu et al. submitted).

Physical measurements

Elemental analyses were carried out with a VARI-EL elemental analyzer. IR spectra (4000–400 cm^{-1}) were recorded using a Shimadzu Fourier transform IR-8300 spectrometer in KBr disks. The kinetic studies of the PTP1B inhibition were recorded with a Hewlett-Packard HP-8453 Chemstation spectrophotometer. Electrospray ionization mass spectra were recorded with a Quattro Micro API instrument (Waters, USA) in methanol solution. Fluorescence emission spectra were recorded on a Cary Eclipse Spectrophotometer (Varian, USA). Bioactivity assays of the compounds were carried out on a Bio-RAD model 550 microplate reader.

Preparation of the vanadyl complex $Na_2[VO(Glu)_2(CH_3OH)]H_2O$ (**1**·H_2O)

$VOSO_4\cdot 3H_2O$ (2.0 mmol) was added slowly to an aqueous/methanol (3:1) solution of glutamic acid (40.0 mmol) with a constant stirring. A 2 M NaOH solution was then added dropwise to maintain pH of the reaction mixture to ~7. After being refluxed for 3 h, the reaction mixture was cooled down to room temperature and subjected to rotary evaporation. Absolute methanol was then added and dark green precipitates were separated by filtration. The products were washed with absolute ethanol and ether, respectively, and then dried in a vacuo desiccator overnight. Element analysis: calcd. (%) for **1**·H_2O: C 29.15, H 4.45, N 6.18; found (%): C 29.17, H 4.96, N 6.27; formula weight (**1**, $Na_2[C_{11}H_{18}N_2O_{10}V]$: 435.02. Electrospray ionization mass spectrometry in positive ion mode (ESI–MS, *m/z*): found: 261.17 (100%), 305.17 (76%), 393.25 (12%), 437.25 (22%); calcd: ([**1**-2Na^++2H^+]$_2$ + 3H^+) 261.71, ([**1**]$_2$ + 2Na^++H^+) 305.68, ([**1**-2Na^++2H^+]$_2$ + 1H^+) 393.07, ([**1**] + H^+) 437.03. IR: see Table 1.

Potentiometric titrations

pH-potentiometric titrations were performed to probe the species formed in aqueous solution. The protonation constants of glutamic acid and the stability constants of the complexes of $VOSO_4$ with ligands

Table 1 IR peaks (cm^{-1}) and assigns of complex **1**, H_2Glu and $VOSO_4{\cdot}3H_2O$

Modes	**1**	H_2Glu	$VOSO_4{\cdot}3H_2O$
υ_{O-H}	–	3566(−COOH)	3471–3363(H_2O)
υ_{N-H}	3412	3266	–
υ_{C-H}	3005	2930, 2892	–
$\upsilon_{O-H(-COOH)\ H\text{-}bond}$	–	2636	–
$\upsilon_{-NH3(+)}$	–	2438, 2306	–
$\delta_{-NH3(+)}$	–	2225, 2115, 2065	–
δ_{COO-}	–	1906, 1857	–
$\upsilon_{C=O\ in\ -COOH}$	–	1752	–
$\upsilon_{C=O\ in\ -COO(-)}$	1713	1711	–
υ_{C-C}, δ_{N-H}	1636	–	1634(δ_{H2O})
$\upsilon_{asCOO(-)}$, $\delta_{-NH3(+)}$	1553	1534, 1492	–
δ_{C-H}, δ_{O-H}	1416	1426	–
υ_{sCOO-},δ_{COO-}	1362	1334	–
υ_{C-N}	1223	1219, 1117	–
$\upsilon_{sSO4(2-)}$	–	–	1136, 1050, 608
$\upsilon_{V=O}$	972	–	993
δ_{NH2}	807, 710	678, 611	–
υ_{V-N}	532	–	–
υ_{V-O}	421	–	–

were determined by pH-potentiometric titrations of 40-ml samples. High-purity nitrogen gas was used to remove carbon dioxide and molecular oxygen from samples and to provide an inert gas atmosphere during all measurements. Measurements of the pH values were carried out at 298 ± 0.1 K and at a constant ionic strength of 0.1 M NaCl on a PHS-3TC pH meter with a combined glass electrode. The electrode was calibrated by standard buffer solutions. The titrations were performed with a carbonate-free NaOH solution of known concentration (0.0967 M) by using a microsyringe under a nitrogen atmosphere in a jacketed vessel. The protonation constants of glutamic acid and the equilibrium constants of the complexes were calculated with the aid of the SUPERQUAD program (Gans et al. 1985). The overall formation constant of the complex is denoted as the logarithm of $\beta_{pqr} = [VO_pGlu_qH_r]/[VO]^p[Glu]^q[H]^r$. The conventional notation has been used: negative indices for H in the formulas indicate either the dissociation of groups which do not deprotonate in the absence of VO^{2+} coordination or hydroxo ligands. The following hydroxo species of VO^{2+} were taken into account in the calculations: $[VO(OH)]^+$ (log $\beta_{10-1} = -5.94$) and $[(VO)_2(OH)_2]^{2+}$ (log $\beta_{20-2} = -6.95$) (Gyurcsik et al. 2001), $[VO(OH)_3]^-$ (log $\beta_{10-3} = -18.0$) and $[(VO)_2(OH)_5]^-$ (log $\beta_{20-5} = -22.0$) (Chruscinska et al. 2008). For Glu, more than 160 data points in the pH range of 2.70–11.50 were used for subsequent analysis; and for VO-Glu, more than 260 data points in the pH range of 2.72–11.29 were used.

Protein tyrosine phosphatase inhibition assays

Kinetics analysis and the inhibitory effects of the vanadium complex against the four PTPs were measured similarly as described previously, using *p*-nitrophenol phosphate (*p*NPP) as the substrate (Yuan et al. 2009; Wang et al. 2010). Briefly, the assays were performed on a 96-well plate in 20 mM MOPS buffer, pH 7.2, containing 50 mM NaCl and 2 mM GSH. The PTPs were diluted to final concentrations of 60, 250, 180, and 200 nM for PTP1B, TCPTP, HePTP, and SHP-1, respectively. 10 µl of the complex at various concentrations was mixed with an enzyme solution (83 µl) for 5 min. Then 2 µl of *p*NPP (0.1 M) substrate was added. After incubation for 30 min at room temperature, the assays were terminated by the addition of 5 µl of 2 M NaOH. The A_{405} was measured on a microplate reader. IC_{50} values were obtained by fitting the concentration-dependent inhibition curves using the Origin program (OriginLab, Northampton, MA).

All data points were carried out in triplicates. Solutions of the oxovanadium complexes were all freshly prepared before each experiment.

The inhibiting kinetic analysis were carried out according to the Lineweaver–Burk plot analysis. Phosphatase activities were measured at a fixed enzyme (PTP1B) concentration while concentrations of the substrate (*p*NPP) and the inhibitor (complex **1**) were varied. The data were fitted using Origin program to generate the Lineweaver–Burk plot.

Fluorescence spectroscopy

Fluorescence emission spectra were recorded on a Cary Eclipse spectrophotometer (Varian, USA) with slit widths 5 nm and excitation wavelength 282 nm. For titration experiments, aliquots of the vanadyl complex (**1**) were added to a PTP1B solution (2 ml, in 20 mM MOPS, 500 mM NaCl, pH 7.2). The mixture was left to equilibrate for 5 min at 298 or 310 K. Fluorescence emission spectra were recorded over the range 290–600 nm.

Results and discussion

Synthesis and characterization of complex **1**

Excessive ligand was employed in the starting materials for the preparation of complex **1**. The element analysis data suggest a chemical formula of **1** as $Na_2[VO(Glu)_2(CH_3OH)]$. The composition was further supported by the electrospray ionization mass spectrometry data (see experimental section) which indicate the presence of monomer and dimer species of complex **1** in solution. Crystallization trials for **1** were not successful. To probe the coordination mode in complex **1**, IR experiments were carried out. The IR spectra for the starting materials, $VOSO_4{\cdot}3H_2O$ and glutamic acid, were also measured for comparison (see Table 1). The assignments of the $\upsilon_{V=O}$, υ_{N-H}, υ_{C-H}, $\upsilon_{C=O}$, υ_{C-C}, δ_{N-H}, $\upsilon_{asCOO(-)}$, $\delta_{-NH3(+)}$, δ_{C-H}, δ_{O-H}, $\upsilon s_{COO(-)}$, $\delta_{COO(-)}$, υ_{C-N}, δ_{NH2}, υ_{V-N}, υ_{V-O} vibrations were made according to published work (SDBS 2010; Yuan et al. 2009; Gao et al. 2009; Zamian et al. 1995). Complex **1** exhibits the characteristic peak for VO^{2+} stretch vibration at approximately 972 cm^{-1}, which was shifted by 21 cm^{-1} compared to that of $VOSO_4{\cdot}3H_2O$, suggesting that the vanadium atom was in a hexacoordinated environment (Mondal et al. 1998). The 532 and 421 cm^{-1} regions belong mainly to "metal–ligand" vibrations, namely, assigned to ν_{V-N} and ν_{V-O} modes (Marques et al. 2007; Zamian et al. 1995). Compare to those in the free Glu, major changes occurred for the stretches and vibrations associated with the amino group (υ_{N-H}, $\upsilon_{-NH3(+)}$, and $\delta_{-NH3(+)}$), suggesting a coordination involving the amino group in Glu. Major perturbations also occurred for the stretching frequencies of C=O in the carboxylate group of Glu, suggesting the coordination of the carboxylic group oxygen to vanadium or sodium cations. Thus, the coordination of the center ion V(IV) in **1** is likely to be VN_2O_4 in a distorted octahedron geometry with two nitrogen atoms and two oxygen atoms from the chelating Glu ligands, one double bond VO and one more oxygen atom from methanol. Taking together, the proposed structure of complex **1** is shown in Scheme 1.

Speciation in aqueous solution

To obtain information about the species of complex **1** formed in aqueous solution, which is relevant to their bioactivities, potentiometric titrations were performed for the system of VO^{2+} cation and glutamic acid at an ionic strength of 0.1 M NaCl. As a preliminary step for studying the VO^{2+}–Glu system, the protonation constants of glutamic acid were determined and the estimated pK_a values were 3.92(5) and 9.67(3). Both values were in agreement with previous reports (Lide 2008; Patel et al. 2003). The stability constants of the hydroxo complexes of VO^{2+} were cited from the literatures (Henry et al. 1973; Davis 1938; Chruscinska et al. 2008). Then the titration curves for the binary systems of VO^{2+}–Glu (1:2) were analyzed. The fitted curve is tallied well with the titration curve (Fig. 1A). The species distribution diagram as a function of pH is shown in Fig. 1B and Table 2. The distribution curves suggest that the oxovanadium species $[(VO)(Glu)_2H_{-1}]$ is the

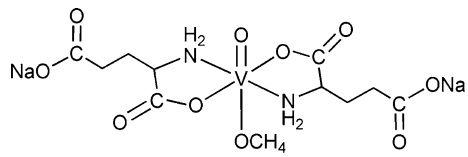

Scheme 1 The schematic structure of complex **1**

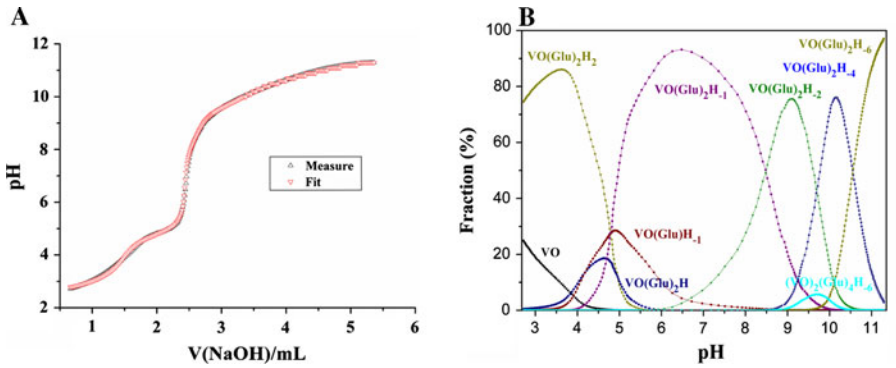

Fig. 1 **A** Titration and fitted curves of VO–Glu system in aqueous solution, **B** Species distribution as a function of pH for the VO–Glu system $[H_2Glu] = 1.5 \times 10^{-3}$ M, $[VO^{2+}] = 0.75 \times 10^{-3}$ M

Table 2 pK_a values of H_2Glu and stability constants for the complexes

Species	pK_a or log(β)
H_2Glu	3.92(5), 9.67(3)
$(VO)(Glu)_2H_2$	29.04(9)
$(VO)(Glu)_2H$	24.07(17)
$(VO)(Glu)H_{-1}$	6.06(16)
$(VO)(Glu)_2H_{-1}$	14.72(8)
$(VO)(Glu)_2H_{-2}$	6.29(9)
$(VO)(Glu)_2H_{-4}$	−13.07(9)
$(VO)(Glu)_2H_{-6}$	−34.21(9)
$(VO)_2(Glu)_4H_{-6}$	−4.12(23)

predominant species over pH 5–8, with a small amount of $[(VO)(Glu)_2H_{-2}]$. The two species are totally about 98% in the pH range of 7.0–7.4. This result is consistent with the conclusion of a previous report that the $[(VO)(Glu)_2H_{-1}]$ species was dominant near neutral pH at high molar ratio of Glu/V(>30) studied by ESR, CD, and potentiometric titration (Costa Pessoa et al. 1992).

PTP inhibition studies

The inhibitory effects of complex **1** against the four PTPs (PTP1B, TcPTP, HePTP, and SHP-1) were investigated (Fig. 2). As seen, complex **1** potently inhibits all the PTPs tested, with IC_{50} of 0.29, 0.24, 0.37, 0.21 μM for PTP1B, TCPTP, HEPTP, and SHP-1, respectively. Little selectivity for the 4 PTPs was observed for complex **1**. This is in contrast to that of the ternary oxovanadium(IV) complexes of ONO donor Schiff base and polypyridyl derivatives which show good selectivity to PTP1B (Yuan et al. 2009, 2010). These results indicate that the structure of the ligands associated with vanadium has an effect on the selectivity of the vanadium complex for different PTPs.

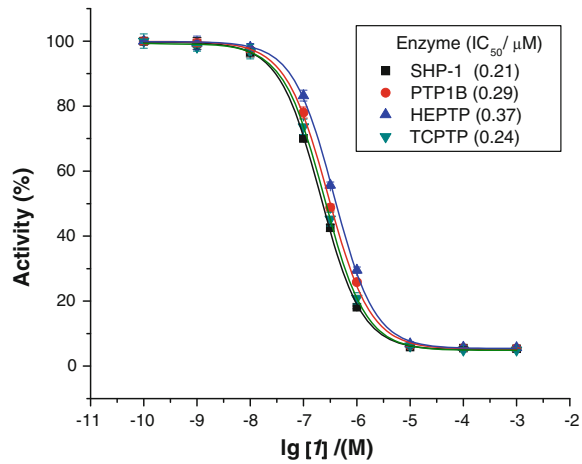

Fig. 2 Concentration-dependent inhibitions of four tyrosine phosphatases by complex **1**. The *inset* shows IC_{50} values

In order to evaluate the inhibition mode of complex **1** on PTP, further kinetic analysis using Lineweaver–Burk plot was carried out as described in the experimental section. The Lineweaver–Burk plot (Fig. 3) give a family of lines intercepting on the 1/*v* axis, suggesting a typical competitive inhibition.

Fluorescence study on the interaction between PTP1B and complex **1**

We further investigated the interactions between PTP1B and **1** by fluorescence spectroscopy. As shown in Fig. 4a, with the addition of **1**, the

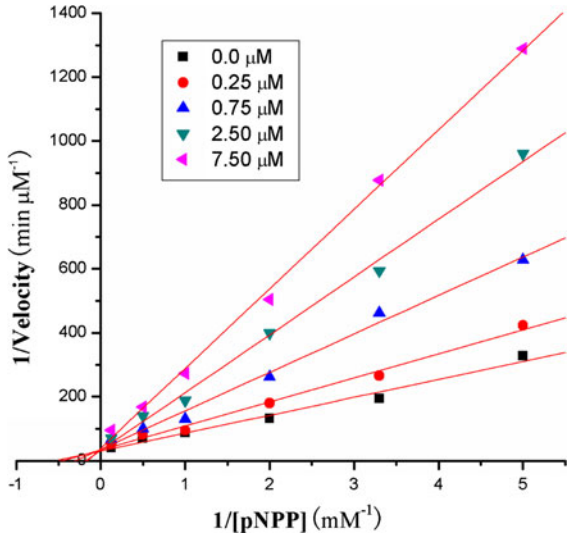

Fig. 3 Lineweaver–Burk plot of $1/v$ (min μM^{-1}) versus $1/[p\text{NPP}]$ (mM^{-1}) at five fixed concentrations of complex **1**

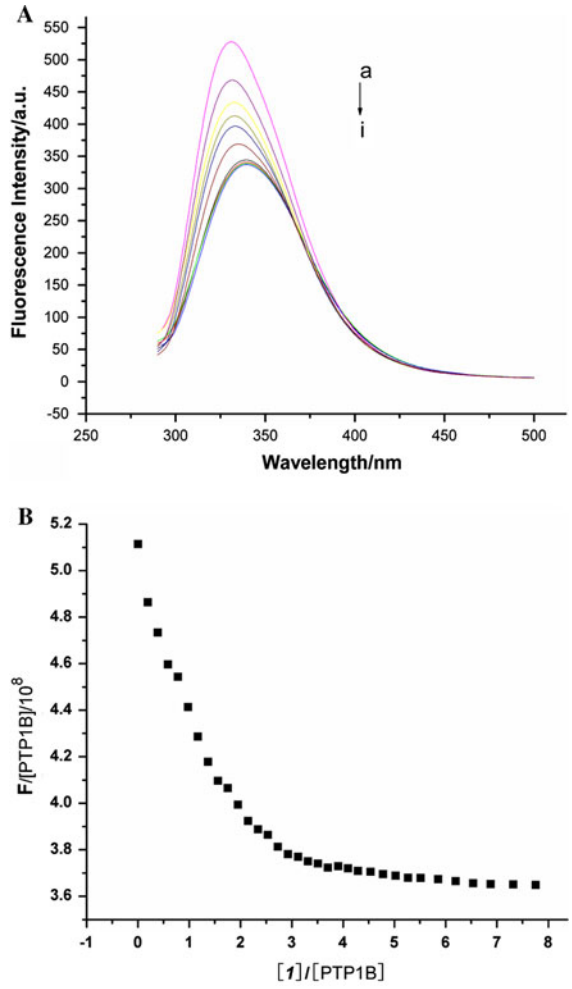

Fig. 4 **A** Fluorescence emission spectra of the titration of PTP1B with **1** in 20 mM MOPS, 500 mM NaCl, pH 7.2 at 298 K. [PTP1B] = 1.0 μM, [**1**]/[PTP1B] = 0 (*a*), 0.25 (*b*), 0.5 (*c*), 0.75 (*d*), 1.0 (*e*), 2.0 (*f*), 4.0 (*g*), 5.0 (*f*), 6.0 (*g*), 7.0 (*h*), 8.0 (*i*). **B** A plot of the intensities of emission at 331 nm against the ratio [**1**]/[PTP1B] at 298 K

fluorescence emission peak of PTP1B at 331 nm was gradually quenched, accompanied by a red shift to 339 nm. These spectroscopic changes suggest a specific binding between **1** and PTP1B. The plot of the fluorescent intensity at 331 nm versus the molar ratio of [**1**]/[PTP1B] (Fig. 4b) suggests a stoichiometry of 2:1 when complex **1** binding to PTP1B. This implies that PTP1B has 2 binding sites for **1**. It is known that PTP1B contains two phosphate binding sites, both being able to bind inhibitors of phosphate analogues (Puius et al. 1997; Salmeen et al. 2000). Thus it is possible that both the phosphate binding sites on PTP1B may bind **1**.

The fluorescence quenching data were further analyzed by the well known Stern–Volmer equation:

$$\frac{F_0}{F} = 1 + k_q \times \tau_0 \times [Q] = 1 + k_{sv} \times [Q] \qquad (1)$$

where F_0 and F are the fluorescence intensities of PTP1B in the absence and presence of complex **1**, respectively, k_q the bimolecular quenching rate constant in $M^{-1}{\cdot}s^{-1}$, τ_0 the lifetime of the fluorophore in the absence of a quencher, k_{sv} the Stern–Volmer quenching constant in M^{-1}, and $[Q]$ the molar concentration of the respective quencher. Generally, τ_0 is about (10^{-8} s) for biopolymer (Ding et al. 2009). As shown in Fig. 5, the Stern–Volmer plots show that the Stern–Volmer quenching constant (the slope, k_{sv}) decreases with increasing temperature; and the values of k_q (1.6×10^{13} l mol^{-1} s^{-1} and 9.7×10^{12} l mol^{-1} s^{-1} at 298 and 310 K, respectively) are much greater than 2.0×10^{10} l mol^{-1} s^{-1}, indicating that the quenching mechanism of PTP1B by complex **1** is not initiated by dynamic collision but by static quenching interactions, i.e., the formation of complex between **1** and PTP1B (Guo et al. 1996; Ding et al. 2009).

For static quenching interactions, the cumulative binding constant is calculated from the following Eq. 2 (Wang et al. 2009):

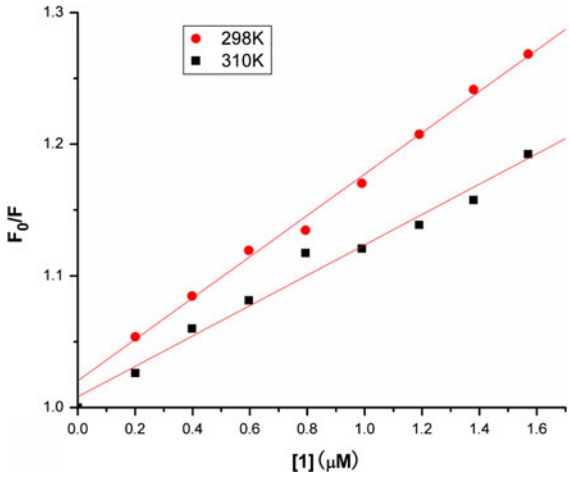

Fig. 5 Stern–Volmer plots for the quenching of PTP1B by **1** at 298 and 310 K

$$\log \frac{[C_{PTP1B}]_b}{[C_{PTP1B}]_u} = \log K + n \log[C_1]_u \quad (2)$$

where $[C_{PTP1B}]_b$ is molar concentration of PTP1B with a quencher bound and $[C_{PTP1B}]_u$ is molar concentration of free PTP1B (with no quencher bound), K the cumulative binding constant, n the number of binding sites on PTP1B, and $[C_1]_u$ the molar concentration of free compound **1**. The calculated cumulative binding constants from the data were $K = 5.13 \times 10^{11}$ at 298 K and $K = 3.28 \times 10^{11}$ at 310 K, respectively.

Usually, thermodynamic parameters, enthalpy change (ΔH) and entropy change (ΔS) are significant for confirming the action force. When the temperature changes at a modest range, ΔH could be considered as a constant. The thermodynamic parameters can be determined from Eq. 3 which is deduced from Van't Hoff equation

$$\ln \frac{K_2}{K_1} = \frac{\Delta H}{R}\left(\frac{T_2 - T_1}{T_1 \times T_2}\right). \quad (3)$$

Gibbs free energy change (ΔG) can be obtained from Eq. 4

$$\Delta G = -RT \ln K = \Delta H - T \times \Delta S \quad (4)$$

where R is the gas constant.

The thermodynamic parameters of this binding interaction are shown in Table 3. The negative ΔH, ΔG and positive ΔS values indicate that the formation of PTP1B-**1** complex was a spontaneous and exothermic reaction. Ross and Subramanian (1981) have characterized the sign and magnitude of the thermodynamic parameter associated with various individual kinds of interactions that may take place in protein association processes. A positive ΔS value is frequently taken as typical evidence for hydrophobic interactions. Negative ΔH values indicate that there are hydrogen bonds and van der Waals force in the binding.

Table 3 Thermodynamic parameters of PTP1B complexing with compound **1**

T(K)	298	310
K	5.13×10^{11}	3.28×10^{11}
ΔG (kJ mol^{-1})	−66.80	−68.34
ΔH (kJ mol^{-1})	−28.63	−28.63
ΔS (J K^{-1} mol^{-1})	128.1	128.1

Conclusion

In summary, we have synthesized and characterized an oxovanadium complex of glutamic acid, $Na_2[VO(Glu)_2(CH_3OH)]\cdot H_2O$ (**1**·H_2O), and investigated its inhibitory effects on 4 PTPs (PTP1B, TCPTP, HePTP, and SHP-1). At physiological relevant pH values, $(VO)(Glu)_2$ species are the dominant species of complex **1** in aqueous solution. Complex **1** displayed potent inhibition against the four PTPs with IC_{50} from 0.21 to 0.37 μM with little selectivity. The complex binds to PTP1B with the formation of a 2:1 complex and inhibits PTP1B competitively, with cumulative binding constants of 5.13×10^{11} and 3.28×10^{11} at 298 and 310 K, respectively. The data presented here suggest that biologically available small ligands such as glutamic acid may form stable complexes with vanadium(IV) under physiological relevant conditions. These complexes may inhibit PTPs potently and thus are relevant to the bioactivities of vanadium-based drugs. When vanadium complexes enter the body, ligand exchanging with biologically available small ligands may occur and this process may alter the bioactivity (e.g., PTP inhibition potency) of the original complexes. Therefore the interactions with bioavailable small ligands with vanadium need to be considered when designing vanadium-based anti-diabetic drugs and evaluating in vivo data.

Acknowledgments This work was financially supported by the National Natural Science Foundation of China (Grant no. 20471033), the China Scholarship Council, the Province Natural Science Foundation of Shanxi Province of China (Grant nos. 20051013, 2010011011-2), the Overseas Returned Scholar Foundation of Shanxi Province of China in 2008 and the University of Massachusetts, Dartmouth, USA.

References

Alal PJ, Gonneville L, Hillman M, Becker-Pasha M, Yue EW, Douty B, Wayland B, Polam P, Crawley ML, McLaughlin E, Sparks RB, Glass B, Takvorian A, Combs AP, Burn TC, Hollis GF, Wynn R (2006) Structural insights into the design of nonpeptidic isothiazolidinone-containing inhibitors of protein-tyrosine phosphatase 1B. J Biol Chem 281:38013–38021

Andersen JN, Jansen PG, Echwald SM, Mortensen OH, Fukada T, Vecchio RD, Tonks NK, Møller NPH (2004) A genomic perspective on protein tyrosine phosphatases: gene structure, pseudogenes, and genetic disease linkage. FASEB J 18:8–30

Arena S, Benvenutis S, Bardellia A (2005) Genetic analysis of the kinome and phosphatome in cancer. Cell Mol Life Sci 62:2092–2099

Byon JC, Kusari AB, Kusari J (1998) Protein-tyrosine phosphatase-1B acts as a negative regulator of insulin signal transduction. Mol Cell Biochem 182:101–108

Chruscinska EL, Sanna D, Garribba E, Micera G (2008) Potentiometric, spectroscopic, electrochemical and DFT characterization of oxovanadium(IV) complexes formed by citrate and tartrates in aqueous solution at high ligand to metal molar ratios: the effects of the trigonal bipyramidal distortion in bis-chelated species and biological implications. Dalton Trans 4903–4916

Costa Pessoa J, Antunest JL, Vilas Boas LF, Gillard RD (1992) Oxovanadium(IV) and amino acids-V. The system L-glutamic acid + VO^{2+}; a potentiometric and spectroscopic study. Polyhedron 11(12):1449–1461

Crans DC, Smee JJ, Gaidamauskas E, Yang L (2004) The chemistry and biochemistry of vanadium and the biological activities exerted by vanadium compounds. Chem Rev 104:849–902

Davis CW (1938) The extent of dissociation of salts in water. part VIII. An equation for the mean ionic activity coefficient of an electrolyte in water, and a revision of the dissociation constants of some sulphates. J Chem Soc 2093–2098

Ding F, Zhao G, Huang J, Sun Y, Zhang L (2009) Fluorescence spectroscopic investigation of the interaction between chloramphenicol and lysozyme. Eur J Med Chem 44: 4083–4089

Elchebly M, Payette P, Michaliszyn E, Cromlish W, Collins S, Loy AL, Normandin D, Cheng A, Himms-Hagen J, Chan CC, Ramachandran C, Gresser MJ, Tremblay ML, Kennedy BP (1999) Increased insulin sensitivity and obesity resistance in mice lacking the protein tyrosine phosphatase-1B gene. Science 283:1544–1548

Gans P, Sabatini A, Vacca A (1985) SUPERQUAD: an improved general program for computation of formation constants from potentiometric data. J Chem Soc Dalton Trans 1195–1200

Gao XL, Lu LP, Zhu ML, Yuan CX, Ma JF, Fu XQ (2009) Inhibitory activities of some oxovanadium complexes with N-heterocyclic ligands against PTP1B/ALP. Acta Chim Sin 67(9):929–936

Guo ML, Yang BS, Yang P (1996) Ethidium bromide as a fluorescent probe for the interaction mode between titanocene dichloride and DNA. Chin Sci Bull 41: 1098–1103

Gyurcsik B, Jakusch T, Kiss T (2001) Oxovanadium(IV) complexes of N-D-gluconylamino acids. J Chem Soc Dalton Trans 1053–1057

Henry RP, Mitchell PCH, Prue JE (1973) Hydrolysis of oxovanadium(IV) ion and stability of its complexes with 1,2-dihydroxybenzenato(2−) ion. J Chem Soc Dalton Trans 1156–1159

Heyliger CE, Tahiliani AG, McNeill JH (1985) Effect of vanadate on elevated blood glucose and depressed cardiac performance of diabetic rats. Science 227:1474–1477

Huyer G, Liu S, Kelly J, Moffat J, Payette P, Kennedy B, Tsaprailis G, Gresser MJ, Ramachandran C (1997) Mechanism of inhibition of protein-tyrosine phosphatases by vanadate and pervanadate. J Biol Chem 272:843–851

Kenner KA, Anyanwu E, Olefsky JM, Kusari J (1996) Protein-tyrosine phosphatase 1B is a negative regulator of insulin- and insulin-like growth factor-I-stimulated signalling. J Biol Chem 271:19810–19816

Klaman LD, Boss O, Peroni OD, Kim JK, Martino JL, Zabolotny LM, Moghal N, Lubkin M, Kim YB, Sharpe AH, Stricker-Krongrad A, Shulman GI, Neel BG, Kahn BB (2000) Increased energy expenditure, decreased adiposity, and tissue-specific insulin sensitivity in protein-tyrosine phosphatase 1B-deficient mice. Mol Cell Biol 20: 5479–5489

Lide DR (2008) Dissociation constants of organic acids and bases. In: CRC handbook of chemistry and physics, 88th edn. (Internet Version). CRC Press/Taylor and Francis, Boca Raton

Lu LP, Gao XL, Wang SX, Liu ZW, Zhu ML, Wu Q, Xing S, Fu XQ, Guo ML. Inhibition of protein tyrosine phosphatases by vanadyl-biguanide complexes. Eur J Med Chem (submitted)

Maccari R, Paoli P, Ottana R, Jacomelli M, Ciurleo R, Manao G, Steindl T, Langer T, Vigorita MG, Camici G (2007) 5-Arylidene-2, 4-thiazolidinediones as inhibitors of protein tyrosine phosphatases. Bioorg Med Chem 15:5137–5149

Marques APD, Dockal ER, Skrobot FC, Rosa ILV (2007) Synthesis, characterization and catalytic study of [*N*, *N*'-bis(3-ethoxysalicylidene)-m-xylylenediamine] oxovanadium(IV) complex. Inorg Chem Commun 10:255–261

McNeill JH, Yuen VG, Dai S, Orvig C (1995) Increased potency of vanadium using organic ligands. Mol Cell Biochem 153:175–180

Mondal S, Rath SP, Rajak KK, Chakravorty A (1998) A family of (*N*-salicylidene-α-amino acidato) vanadate esters incorporating chelated propane-1, 3-diol and glycerol: synthesis, structure, and reaction. Inorg Chem 37(8): 1713–1719

Mukherjee R, Donnay EG, Radomski MA, Miller C, Redfern DA, Gericke A, Damron DS, Brasch NE (2008) Vanadium–vitamin B12 bioconjugates as potential therapeutics for treating diabetes. Chem Commun 3783–3785

Na M, Cui L, Min BS, Bae KH, Yoo JK, Kim BY, Oh WK, Ahn JS (2006) Protein tyrosine phosphatase 1B inhibitory activity of triterpenes isolated from Astilbe Koreana. Bioorg Med Chem Lett 16:3273–3276

Nxumalo F, Glover NR, Tracey AS (1998) Reactions of vanadium(V) complexes of *N*, *N*-dimethylhydroxylamine with sulfur-containing ligands: implications for protein tyrosine phosphatase inhibition. J Biol Inorg Chem 3:534–542

Patel RN, Soni VK, Sharma S, Shukla KK, Pandeya KB (2003) pH-metric and spectrophotometric study of oxovanadium(IV) with aspartic acid, glutamic acid and imidazoles. Oxid Commun 26:358–367

Peters KG, Davis MG, Howard BW, Pokross M, Rastogi V, Diven C, Greis KD, Eby-Wilkens E, Maier M, Evdokimov A, Soper S, Genbauffe FJ (2003) Mechanism of insulin sensitization by BMOV (bis maltolato oxovanadium): unliganded vanadium(VO_4) as the active component. J Inorg Biochem 96:321–330

Posner BI, Faure R, Burgess JW, Bevan AP, Lachance D, Zhang-Sun G, Fantus IG, Ng JB, Hall DA, Lum BS (1994) Peroxovanadium compounds. J Biol Chem 269: 4596–4604

Puius YA, Zhao Y, Sullivan M, Lawrence DS, Almo SC, Zhang ZY (1997) Identification of a second aryl phosphate-binding site in protein-tyrosine phosphatase 1B: a paradigm for inhibitor design. Proc Natl Acad Sci USA 94:13420–13425

Ross PD, Subramanian S (1981) Thermodynamics of protein association reactions: forces contributing to stability. Biochemistry 20:3096–3102

Saltiel AR, Kahn R (2001) Insulin signalling and the regulation of glucose and lipid metabolism. Nature 414:799–806

Salmeen A, Andersen JN, Myers MP, Tonks NK, Barford D (2000) Molecular basis for the dephosphorylation of the activation segment of the insulin receptor by protein tyrosine phosphatase 1B. Mol Cell 6:1401–1412

SDBS Nos 4736, 4628, and 1097; SDBSWeb: http://riodb01.ibase.aist.go.jp/sdbs/ (National Institute of Advanced Industrial Science and Technology, Accessed 9 Jan 2010)

Shrestha S, Bhattarai BRK, Lee H, Cho H (2007) Mono- and disalicylic acid derivatives: PTP1B inhibitors as potential anti-obesity drugs. Bioorg Med Chem 15:6535–6548

Sparks RB, Polam P, Zhu W, Crawley ML, Takvorian A, McLaughlin E, Wei M, Ala PJ, Gonneville L, Taylor N, Li Y, Wynn R, Burn TC, Liu PCC, Combs AP (2007) Benzothiazole benzimidazole (S)-isothiazolidinone derivatives as protein tyrosine phosphatase-1B inhibitors. Bioorg Med Chem Lett 17:736–740

Wang HY, Zhang M, Lv QL, Yue NN, Gong B (2009) Determination of berberine and the study of fluorescence quenching mechanism between berberine and enzyme-catalyzed product. Spectrochim Acta Part A 73:682–686

Wang QM, Lu LP, Yuan CX, Pei K, Liu ZW, Guo ML, Zhu ML (2010) Potent inhibition of protein tyrosine phosphatase 1B by copper complexes: implication to copper toxicity in biological systems. Chem Commun 46: 3547–3549

Winter CL, Lange JS, Davis MG, Gerwe GS, Downs TR, Peters KG, Kasibhatla B (2005) A nonspecific phosphotyrosine phosphatase inhibitor, bis(maltolato)oxovanadium(IV), improves glucose tolerance and prevents diabetes in zucker diabetic fatty rats. Exp Biol Med 230:207–216

Xie J, Seto CT (2007) A two stage click-based library of protein tyrosine phosphatase inhibitors. Bioorg Med Chem 15:458–473

Yuan CX, Lu LP, Gao XL, Wu YB, Yue JJ, Guo ML, Li Y, Fu XQ, Zhu ML (2009) Ternary oxovanadium(IV) complexes of ono-donor schiff base and polypyridyl derivatives as protein tyrosine phosphatase inhibitors: synthesis, characterization, and biological activities. J Biol Inorg Chem 14:841–851

Yuan CX, Lu LP, Wu YB, Liu ZW, Guo ML, Xing S, Fu XQ, Zhu ML (2010) Synthesis, characterization, and protein tyrosine phosphatases inhibition activities of oxovanadium(IV) complexes with schiff base and polypyridyl derivatives. J Inorg Biochem doi:10.1016/j.jinorgbio.2010.05.003

Zamian JR, Dockal ER, Castellano G, Oliva G (1995) Synthesis and characterization of [*N*, *N*'-ethylenebis(3-ethoxysalicylideneaminato)]oxovanadium(IV). Polyhedron 14:2411–2418

Zhang ZY (2001) Protein tyrosine phosphatases: prospects for therapeutics. Curr Opin Chem Biol 5:416–423

Zinker BA, Rondinone CM, Trevillyan JM, Gum RJ, Clampit JE, Waring JF, Xie N, Wilcox D, Jacobson P, Frost L, Kroeger PE, Reilly RM, Koterski S, Opgenorth TJ, Ulrich RG, Crosby S, Butler M, Murray SF, McKay RA, Bhanot S, Monia BP, Jirousek MR (2002) PTP1B antisense oligonucleotide lowers PTP1B protein, normalizes blood glucose, and improves insulin sensitivity in diabetic mice. Proc Natl Acad Sci USA 99:11357–11362